We are IntechOpen, the world's leading publisher of Open Access books Built by scientists, for scientists

6,900
Open access books available

185,000
International authors and editors

200M
Downloads

Our authors are among the

154
Countries delivered to

TOP 1%
most cited scientists

12.2%
Contributors from top 500 universities



WEB OF SCIENCE™

Selection of our books indexed in the Book Citation Index in Web of Science™ Core Collection (BKCI)

Interested in publishing with us?
Contact book.department@intechopen.com

Numbers displayed above are based on latest data collected.
For more information visit www.intechopen.com



Chapter 7

Nondestructive Testing Structural Bridge Identification

Ahmet Can Altunışık

Additional information is available at the end of the chapter

http://dx.doi.org/10.5772/64288

Abstract

The bridges are one of the most important engineering structures. Determination of the bridge responses during their service life has gained great importance using nondestructive test methods with the changing of aims, usages, environmental conditions, material deteriorations by time, and damages during some dramatical events. This chapter presents the nondestructive experimental measurement test results of the bridges for structural identification. Ten different bridges, which have different type and carrier systems, such as historical masonry arch bridges, long span concrete highway bridges, base isolated bridges, footbridges, steel bridges, and old riveted bridges, are selected for numerical examples. The measurements are conducted under environmental excitations of pedestrian movement, traffic, wind-induced vibration, and the response signals are collected using uniaxial- and triaxial-sensitive seismic accelerometers. Operational modal analysis or ambient vibration tests are performed to extract the dynamic characteristics such as natural frequencies, mode shapes, and damping rations using enhanced frequency domain decomposition method in the frequency domain and stochastic subspace identification method in the time domain. It is demonstrated that the ambient vibration measurements are enough to identify the most significant modes of all bridge types.

Keywords: ambient vibration test, dynamic characteristics, nondestructive test methods, operational modal analysis

1. Introduction

The bridges, which link past to present and age gracefully, are one of the most important engineering structures. The bridges with different characteristics, thanks to their views, effects, and feelings during passing on, holds around and locations bring together the people for ages. In early applications, the bridges were designed as short span and narrow with stone and wood

INTECH
open science | open minds

© 2016 The Author(s). Licensee InTech. This chapter is distributed under the terms of the Creative Commons Attribution License (http://creativecommons.org/licenses/by/3.0), which permits unrestricted use, distribution, and reproduction in any medium, provided the original work is properly cited. CC BY

materials, and be able to carry light loads. But, nowadays, these conventional bridges have been replaced to steel and reinforced concrete.

There are various bridge types constructed during the last century according to the carrier system type, span lengths, and material properties such as masonry arch bridges, long span concrete/steel/composite highway bridges, base isolated bridges, footbridges, steel bridges, suspension bridges, cable-stayed bridges, and wooden/timber bridges. Masonry bridges have been built worldwide for social, economic, and strategic purposes. Originally intended to carry only pedestrian and horse-drawn vehicles, many of these historical bridges currently serve as critical components of transportation systems and, thus, must withstand significantly larger loads. Among various types of civil engineering structures, long span highway bridges, which are commonly used for passing large rivers, dam reservoirs, and deep valleys, attract the greatest interest for study particularly in terms of structural performance. Footbridges are generally situated to allow pedestrians to cross water or railways in areas where there are no nearby roads to necessitate a road bridge, and also across busy roads to let pedestrians cross safely without slowing down the traffic. Steel offers many advantages to the bridge builder, not only the material itself, but also its broad architectural possibilities such as high strength-to-weight ratio, high-quality material, speed of construction, versatility, modifications, recycling, durability, and aesthetics. Suspension and cable-stayed bridges are widely used across long spans (>550 m) and give rise to the usage of domains under the bridge. For this reason, the uses of suspension and cable-stayed bridges have increased recently. Wood is one of the most used and common materials for bridge constructions from the ancient times when humans first started finding ways on how to cross rivers and hard terrains.

Determination of dynamic response of bridges under static and dynamic loads, such as wind, earthquake, or traffic, is very complex and requires special studies. Finite element method has been widely used in civil engineering application since 1950s. Static, dynamic, linear, and nonlinear behavior can be obtained and illustrated using this method. It is generally expected that finite element models (FEMs) based on technical design data and engineering judgments can yield reliable simulation. However, because of modeling uncertainties, these models often cannot predict dynamic characteristics with the required level of accuracy. This raises the need for verification of finite element models using nondestructive experimental measurement tests.

There are two basically different methods available to experimentally identify the dynamic system parameters of a structure: experimental modal analysis (EMA) and operational modal analysis (OMA). In the EMA, the structure is excited by known input forces and the structural behavior is evaluated. In the OMA, the ambient vibrations such as vehicle load, wind, or wave loads have been used to actuate the structures. Heavy forced excitations may become expensive and sometimes may cause damage to the structure. Ambient excitations and their combination are environmental or natural excitations. Structural identification using this method gains the major importance. In this case, only response data of ambient vibrations are measurable while actual loading conditions are unknown. A system identification procedure will therefore need to base itself on output-only data.

It is well accepted that the finite element model updating is used to minimize the differences between analytically and experimentally determined dynamic characteristics by changing

http://dx.doi.org/10.5772/64288

some uncertain parameters such as material properties, boundary conditions, section and connection details, and some additional structural elements and weights. In the finite element model updating, determination of the uncertain parameters and their ratios/values can be decided according to the nondestructive testing methods such as visual inspection, half-cell electrical potential method, Schmidt rebound hammer test, carbonation depth measurement test, permeability test, penetration resistance or Windsor probe test, resistivity measurement, electromagnetic methods, radiographic testing, ultrasonic testing, infrared thermography, ground penetrating radar, radioisotope gauges, acoustics emission, computed tomography, strain sensing, and corrosion rate measurement. The detailed information can be found in the related literature.

2. Modal parameter estimation methods

2.1. Enhanced frequency domain decomposition (EFDD) method

Enhanced frequency domain decomposition (EFDD) method is an extension of frequency domain decomposition (FDD) method which is a basic and easy-to-use method. In this method, modes are simply picked locating the peaks in singular value decomposition plots [1, 2].

In EFDD, the single degree of freedom (SDOF) power spectral density (PSD) function, identified around a peak of resonance, is taken back to the time domain using the Inverse Discrete Fourier Transform. In EFDD method, the relationship between unknown input and measured responses can be expressed as [2, 3]:

$$\left[G_{yy}(jw)\right] = \left[H\{jw\}\right]^{*}\left[G_{xx}\{jw\}\right]\left[H(jw)\right]^{T} \tag{1}$$

where $G_{xx}\{jw\}$ is the PSD matrix of the input, $G_{yy}\{jw\}$ is the PSD matrix of the responses, $H\{jw\}$ is the frequency response function (FRF) matrix, and * and superscript T denote complex conjugate and transpose, respectively. The FRF can be written in partial fraction, i.e., pole/residue form as [4]

$$H\{jw\} = \sum_{k=1}^{n} \frac{R_k}{jw - \lambda_k} + \frac{R_k^*}{jw - \lambda_k^*} \tag{2}$$

where n is the number of modes, λ_k is the pole, and, R_k is the residue. Substituting Eq. (2) into (1), we have

$$G_{yy}(jw) = \sum_{k=1}^{n}\sum_{s=1}^{n}\left[\frac{R_k}{jw - \lambda_k} + \frac{R_k^*}{jw - \lambda_k^*}\right]\left[G_{xx}\{jw\}\right]\left[\frac{R_s}{jw - \lambda_s} + \frac{R_s^*}{jw - \lambda_s^*}\right]^{H} \tag{3}$$

where s is the singular value, superscript H denotes complex conjugate and transpose. Multiplying the two partial fraction factors and making use of the Heaviside partial fraction theorem, the output PSD can be reduced to a pole/residue form as follows:

$$G_{yy}(jw) = \sum_{k=1}^{n} \frac{A_k}{jw - \lambda_k} + \frac{A_k^*}{jw - \lambda_k^*} + \frac{B_k}{-jw - \lambda_k} + \frac{B_k^*}{-jw - \lambda_k^*} \tag{4}$$

where A_k is the kth residue matrix of the output PSD. In the EFDD identification, the first step is to estimate the PSD matrix. The estimation of the output PSD, $G_{yy}(jw)$ known at discrete frequencies $w = w_i$ is then decomposed by taking the SVD of the matrix

$$G_{yy}(jw_i) = U_i S_i U_i^H \tag{5}$$

where the matrix $U_i = [u_{i1}, u_{i2}, \ldots, u_{im}]$ is a unitary matrix holding the singular vectors, u_{ij}, and S_i is a diagonal matrix holding the scalar singular values s_{ij} [4–6].

2.2. Stochastic subspace identification (SSI) method

Stochastic subspace identification (SSI) method is an output-only time domain method that directly works with time data, without the need to convert them to correlations. The model of structural vibrations can be defined by a set of linear, constant coefficient and second-order differential equations [7]:

$$M\ddot{U}(t) + C_2\dot{U}(t) + KU(t) = F(t) = B_2 u(t) \tag{6}$$

where M, C_2, and K are the mass, damping, and stiffness matrices, $F(t)$ is the excitation force, and $U(t)$ is the displacement vector depending on time t. Note that the force vector $F(t)$ is factorized into a matrix B_2 describing the inputs in space and a vector $u(t)$. The equation of dynamic equilibrium (6) will be converted to a more suitable form: the discrete-time stochastic state-space model [7, 8]. With the following definitions

$$x(t) = \begin{pmatrix} U(t) \\ \dot{U}(t) \end{pmatrix},\ A = \begin{pmatrix} 0 & I_{n_2} \\ -M^{-1}K & -M^{-1}C_2 \end{pmatrix},\ B = \begin{pmatrix} 0 \\ M^{-1}B_2 \end{pmatrix} \tag{7}$$

Eq. (6) can be transformed into the state equation

$$\dot{x}(t) = Ax(t) + Bu(t) \tag{8}$$

http://dx.doi.org/10.5772/64288

where A is the state matrix, B is the input matrix, and $x(t)$ is the state vector. If it is assumed that the measurements are evaluated at only one sensor location, and that this sensor can be accelerometer, velocity, or displacement transducer, the observation equation is [9]:

$$y(t) = Cx(t) + Du(t) \tag{9}$$

where C is the output matrix and D is the direct transmission matrix. Eqs. (8) and (9) constitute a continuous-time deterministic state-space model. This is not realistic: measurements are available at discrete time instants $k\Delta t$, $k \in N$ with Δt, the sample time and noise is always influencing the data. After sampling, the state-space model looks like [6]:

$$\begin{aligned} x_{k+1} &= Ax_k + Bu_k \\ y_k &= Cx_k + Du_k \end{aligned} \tag{10}$$

where $x_k = x(k\Delta t)$ is the discrete-time state vector. The stochastic components are included and obtained discrete-time combined deterministic-stochastic state-space model:

$$\begin{aligned} x_{k+1} &= Ax_k + Bu_k + w_k \\ y_k &= Cx_k + Du_k + v_k \end{aligned} \tag{11}$$

where w_k is the process noise due to disturbances and modeling inaccuracies and v_k is the measurement noise due to the sensor inaccuracy. They are both immeasurable vector signals but we assume that they are zero mean, white, and covariance matrices [7]:

$$E\left[\begin{pmatrix} w_p \\ v_p \end{pmatrix}\begin{pmatrix} w_q^T & v_q^T \end{pmatrix}\right] = \begin{pmatrix} Q & S \\ S^T & R \end{pmatrix}\delta_{pq} \tag{12}$$

where E is the expected value operator and δ_{pq} is the Kronecker delta. This is a function of two variables, usually integers, which is 1 if they are equal, and 0 otherwise. It can be written as the symbol δ_{pq}, and treated as a notational shorthand rather than a function:

$$\delta_{pq} = \begin{cases} 1, \; if \;\; p = q \\ 0, \; if \;\; p \neq q \end{cases} \tag{13}$$

The vibration information that is available in structural health monitoring is usually the responses of a structure excited by the operational inputs that are some immeasurable inputs.

It is impossible to distinguish deterministic input u_k from the noise terms w_k, v_k in Eq. (11). If the deterministic input term u_k is modeled by the noise terms w_k, v_k the discrete-time purely stochastic state-space model is obtained:

$$\begin{aligned} x_{k+1} &= Ax_k + w_k \\ y_k &= Cx_k + v_k \end{aligned} \tag{14}$$

Eq. (14) constitutes the basis for the time-domain system identification through operational vibration measurements.

2.3. Modal assurance criterion

The modal assurance criterion (MAC) is defined as a scalar constant relating the degree of consistency (linearity) between one modal and another reference modal vector [10] as follows:

$$MAC = \frac{\left|\{\varnothing_{ai}\}^T \{\varnothing_{ej}\}\right|^2}{\{\varnothing_{ai}\}^T \{\varnothing_{ai}\}\{\varnothing_{ej}\}^T \{\varnothing_{ej}\}} \tag{15}$$

where $\{\emptyset_{ai}\}$ and $\{\emptyset_{ej}\}$ are the modal vectors of *i*th and *j*th for different methods, respectively.

3. Nondestructive testing of bridges

In the content of this chapter, 10 different bridges that have different type and carrier systems are selected as case studies:

- Historical masonry arch bridges (Osmanlı, Mikron, and Şenyuva)
- Long span concrete highway bridges (Kömürhan and Birecik)
- Base isolated bridge (Gülburnu)
- Footbridges (Ortahisar and Akçaabat)
- Steel bridges (Eynel)
- Old riveted bridges (Borçka)

3.1. Historical masonry arch bridges

Historical structures are identity of the communities. They are not only structures, which contain stone, timber, mortar, etc., they also contain the social culture and this is the biggest difference between the new structures. Almost every person is curious about the past and they want to learn some information of their ancestors. So the easiest way to learn about the past is

http://dx.doi.org/10.5772/64288

to examine the historical data and structures. In the last century, people have given more attention to preserve the historical structures. A lot of studies have been carried out for

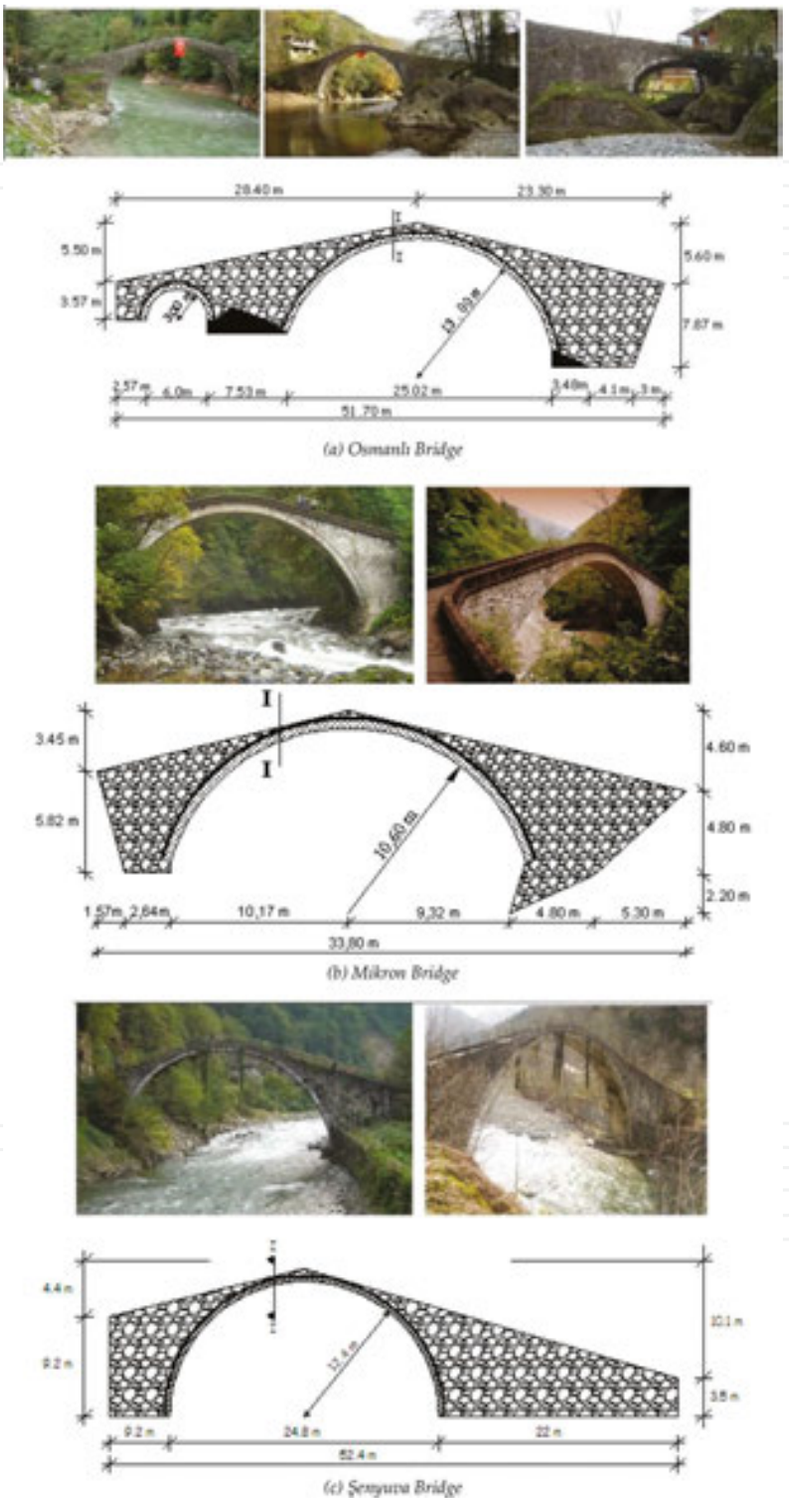


Figure 1. Views of the historical masonry arch bridges with relieve drawings. (a) Osmanlı Bridge, (b) Mikron Bridge, and (c) Şenyuva Bridge.

estimating behavior of these structures and reliable restoration could be made to preserve them for future.

Masonry arch bridges hold an important place in historical structures [11]. They are not complex structures. A stone arch bridge consists of stone blocks and mortar joints. Blocks have high strength in compression and low strength in tension while mortar has generally low strength. Historical masonry arch bridges are vital components of transportation systems in many countries worldwide, ensuring the ready access of goods and services to millions of people [12]. Many of those bridges, which were originally built for the passage of carts, are being used for road and rail vehicles. They demonstrate a surprisingly high load bearing capacity and good durability.

Osmanlı, Mikron, and Şenyuva historical masonry arch bridges constructed in Turkey are selected for example. The Osmanlı historical masonry arch bridge was built in the nineteenth

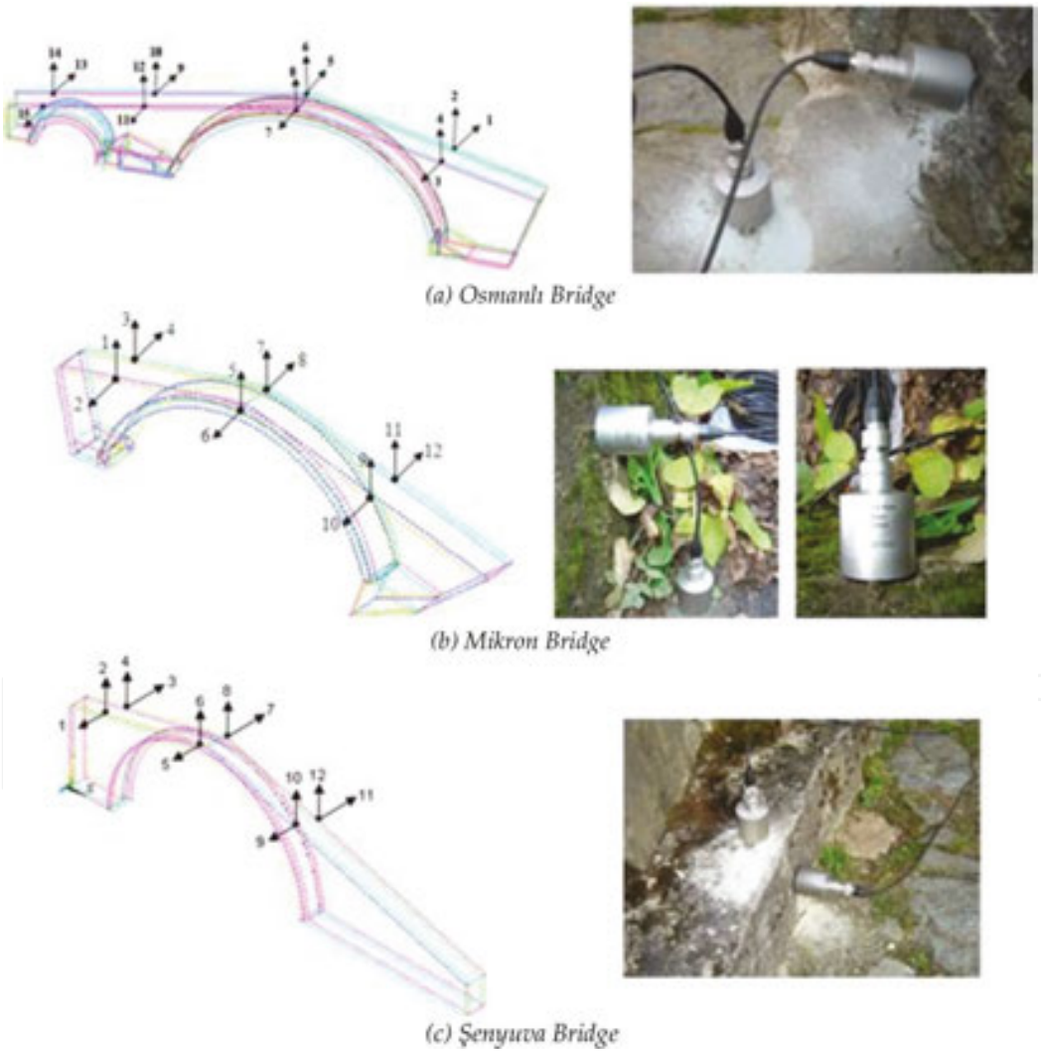


Figure 2. Accelerometer locations and views from the measurements. (a) Osmanlı Bridge, (b) Mikron Bridge, and (c) Şenyuva Bridge.

http://dx.doi.org/10.5772/64288

century. This two-spanned arch bridge has a total length of 51.7 m. The span of each arch is 25.2 and 6 m, and the radius of each arch is 13 and 3m, respectively.

The Mikron historic arch bridge, built in the mid-nineteenth century during the Ottoman Empire, spans the Fırtına River in Rize, Turkey. Cut stone blocks composed the bridge's arches and parapets. In 1998, Turkey's General Directorate for Highways supervised repair of the main structural elements of the bridge (stone arches, side walls, and filler material). The bridge, with a total length of 33.80 m, has two stone, inner and outer semi-circular arches, which have thicknesses of 0.50 and 0.15 m, respectively.

The Şenyuva historical arch bridge built in 1696 by the native population is located on Fırtına Stream in Çamlihemşin, Rize, Turkey. The bridge has a single arch. The total span of bridge is 52.4 m, the span of the bridge arch is 24.8 m, the height of the arch is 12.4 m, and the wide of the deck is 2.5 m. Height of the side walls at both side are 9.2 and 3.5 m, respectively. There are 60 cm × 30 cm dimensional parapets on both sides of the bridge deck. Some views of the bridges with relieve drawings are given in **Figure 1(a–c)**.

Ambient vibration tests were performed under existing environmental condition. B&K 8340 and B&K 3560 experimental measurement equipment were used. PULSE [13] and OMA [14] softwares were used to signal processing and parameter estimations. Accelerometer locations and views from the measurements for each bridge are shown in **Figure 2**.

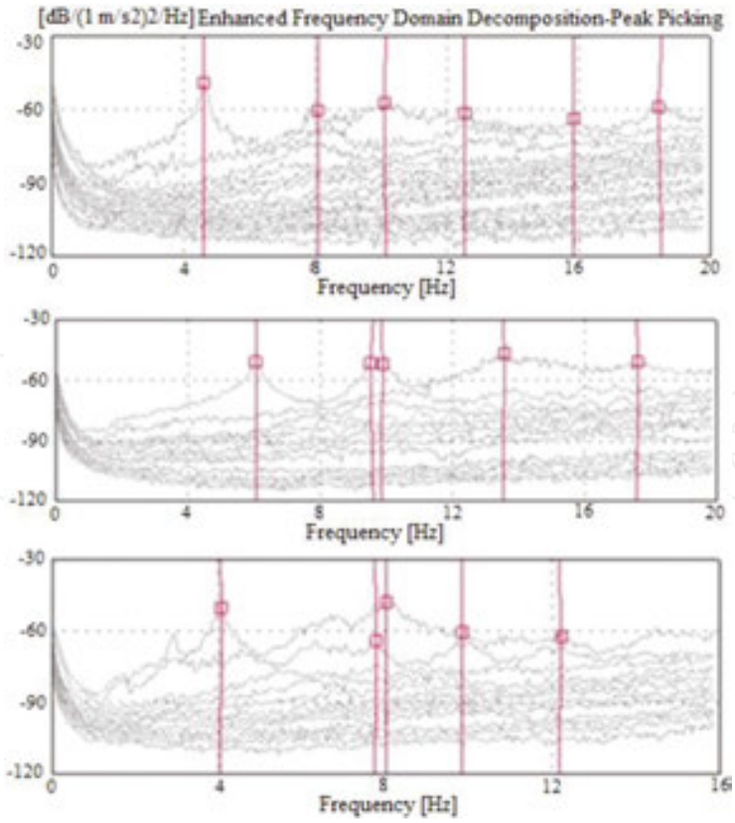


Figure 3. The singular values of spectral density matrices for historical masonry arch bridges.

Accelerometer setups shown in **Figure 2** were used, and measurements were carried out for at least 30 min. The singular values of spectral density matrices are given in **Figure 3**. The dynamic characteristics are given in **Table 1** and **Figure 4**. The first four natural frequencies are obtained between 4 and 14 Hz. The mode shapes occurred as lateral and vertical forms.

Bridges	Natural frequencies (Hz)				Damping ratio (%)			
	1	2	3	4	1	2	3	4
	EFDD method							
Osmanlı	4.640	8.094	9.879	12.340	1.634	1.035	6.157	0.256
Mikron	6.063	9.563	9.906	13.590	1.945	0.967	0.835	0.258
Şenyuva	4.045	7.750	8.020	10.000	2.377	1.318	4.288	0.265
	SSI method							
Osmanlı	4.642	8.325	9.735	11.910	1.634	1.035	6.157	0.256
Mikron	6.065	9.558	10.180	13.590	1.855	0.923	0.815	0.289
Şenyuva	4.066	7.960	8.044	10.100	2.377	1.318	4.288	0.265

Table 1. Experimentally identified natural frequencies and damping ratios.

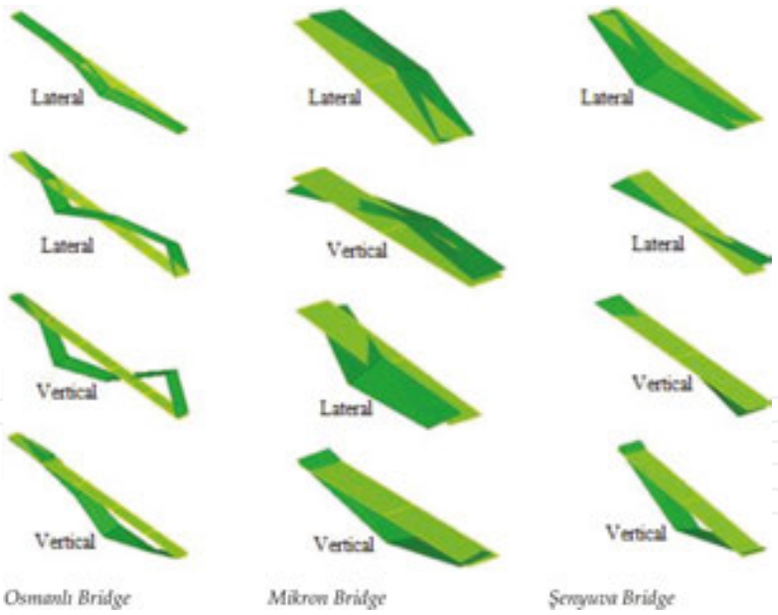


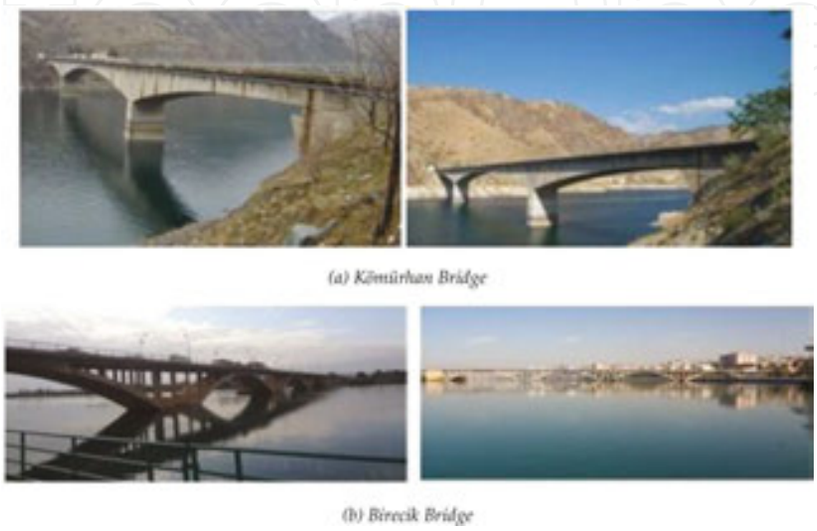
Figure 4. The first four mode shapes of the historical masonry arch bridges.

3.2. Long span concrete highway bridges

Kömürhan and Birecik long span concrete highway bridges constructed in Turkey are selected for example. The bridge deck consists of a main span of 135 m and two side span of 76 m each.

http://dx.doi.org/10.5772/64288

The total bridge length is 287 m and width of the bridge is 11.50 m. The structural system of Kömürhan Highway Bridge consists of deck, columns, side support, and expansion joint. The deck of the bridge was constructed with balanced cantilever and prestressed box beam method. There are two main columns of 59.50 m each. Foundation of the main column is concrete in mass having the dimension of 24 m × 13.5 m and 5 m depth. To combine deck cantilevers, an expansion joint is constituted in the main span of the bridge [16, 17].



(a) Kömürhan Bridge

(b) Birecik Bridge

Figure 5. Some views of the long span concrete highway bridges with relieve drawings. (a) Kömürhan Bridge and (b) Birecik Bridge.

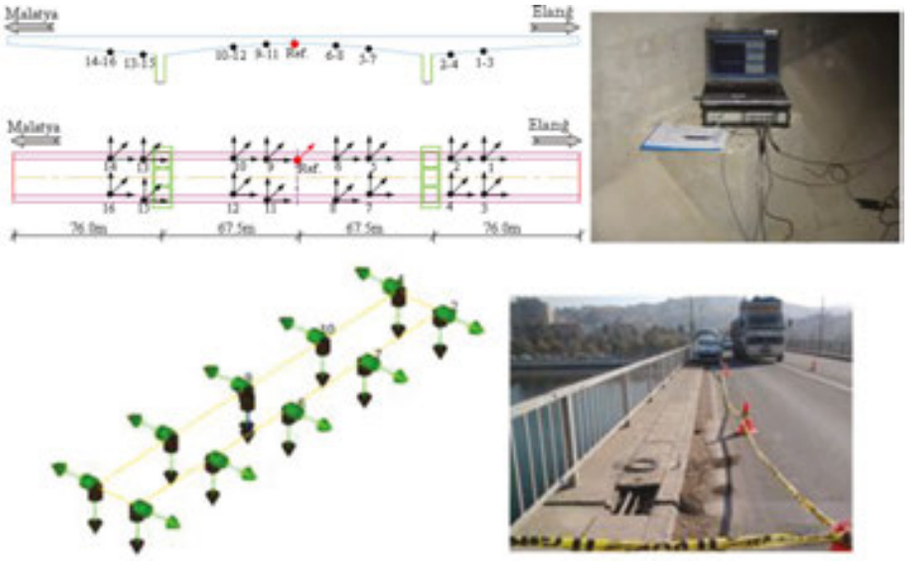


Figure 6. Accelerometer location and views from the measurements.

Birecik Bridge is located 81 km of the Şanlıurfa-Gaziantep state highway over Fırat River in Turkey. The construction of the bridge was started in June 1951 and the bridge was opened to

the traffic in April 1956. The bridge consist of five arches, each arch has a 55 m main span. The total bridge length is 300 m and the width of the bridge is 10 m. The bridge arches have rigid connectivity at middle spans and side supports. But, right and left side of the middle points of slabs are constructed using joints. Columns, beams, arches, decks, and foundations were constructed as reinforced concrete [18]. Some views of the bridges with relieve drawings is given in **Figure 5**. **Figure 6** presents the accelerometer location and views from the measurement. The measurements were carried out for at least 60 min. The singular values of spectral density matrices obtained from vibration data are given in **Figure 7**.

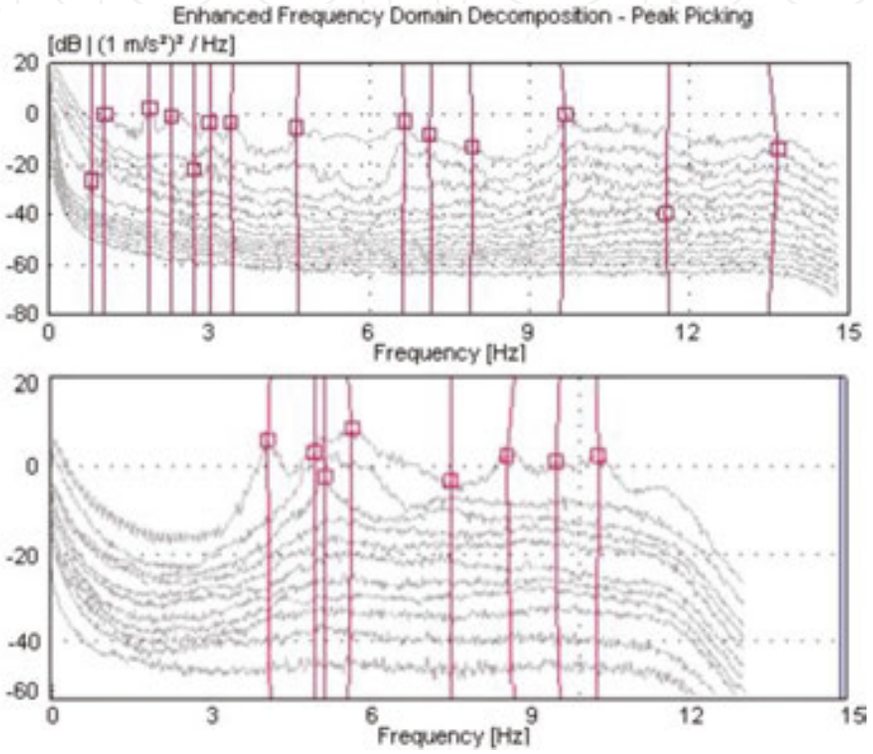


Figure 7. The singular values of spectral density matrices for long span highway bridges.

The dynamic characteristics and related mode shapes are given in **Table 2** and **Figure 8**. The first four natural frequencies are obtained between 0.7 and 2.3 Hz for the Kömürhan Bridge and 2.4 and 4.6 Hz for the Birecik Bridge, respectively. The mode shapes occurred in lateral, vertical, and torsional forms.

Bridges	**EFDD method**							
	Natural frequencies (Hz)				**Damping ratio (%)**			
	1	**2**	**3**	**4**	**1**	**2**	**3**	**4**
Kömürhan	0.788	1.027	1.850	2.291	1.373	1.785	2.057	1.465
Birecik	2.496	3.115	3.378	4.545	4.358	0.899	0.863	0.118

Table 2. Experimentally identified natural frequencies and damping ratios.

http://dx.doi.org/10.5772/64288

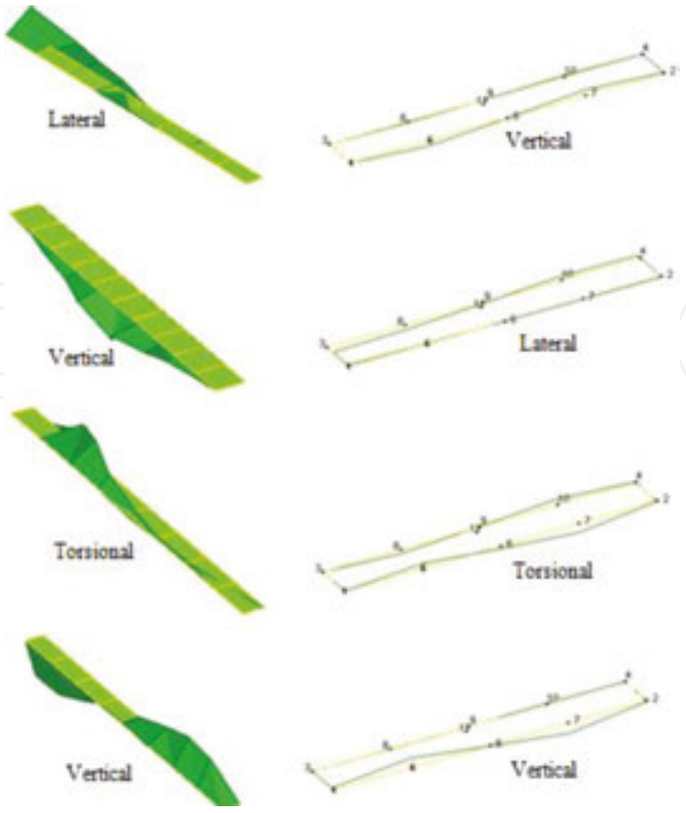


Figure 8. The first four mode shapes of the long span highway bridges.

3.3. Base isolated bridge

Base isolated Gülburnu Highway Bridge constructed in Turkey is selected for example. The construction of the bridge was started in November 2005 and the bridge was opened to the traffic in May 2009. The bridge is twin prestressed concrete box girder structures. The bridge

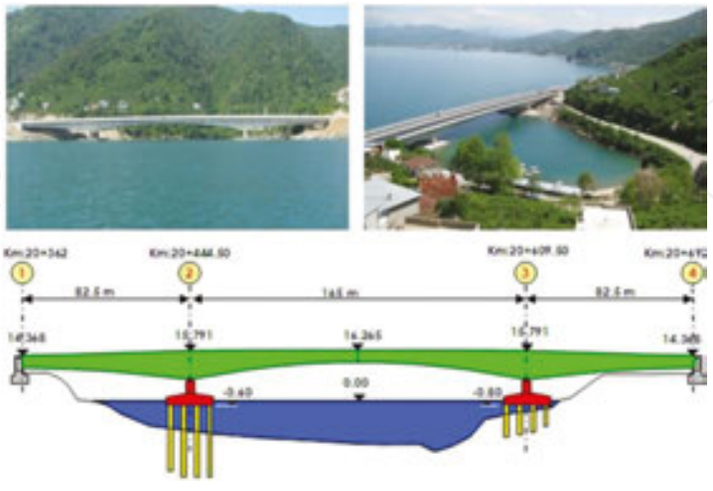


Figure 9. Some views of the base isolated bridge with relieve drawings.

deck consists of a main span of 165 m and two side span of 82.5 m each. The total bridge length is 330 m and the width of the bridge is 30 m. The structural system of the bridge consists of deck, piers, and side support. There are four piers and each has 4.50 m height and 9.00 m × 3.75 m cross-section areas. All piers are footed on the two raft foundation with bored piles. Two abutments that allow longitudinal direction movement only support the superstructure at both sides [19, 20]. Some views of the bridge with relieve drawings is given in **Figure 9**.

Accelerometer locations are shown in **Figure 10**. The measurements were carried out for at least 60 min. The singular values of spectral density matrices obtained from the processing vibration data are given in **Figure 11**.

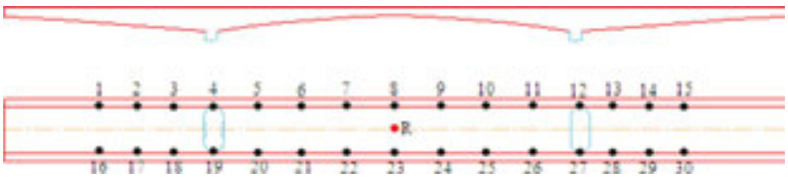


Figure 10. Accelerometer location and views taken from the measurements.

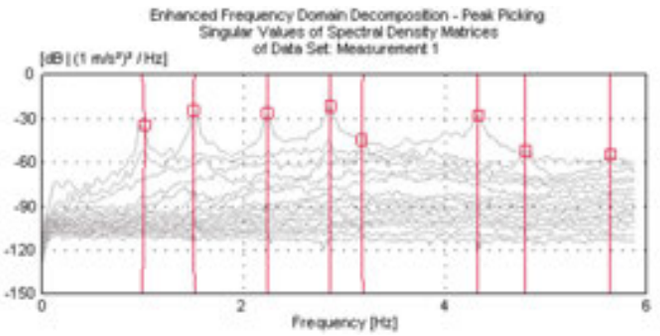


Figure 11. The singular values of spectral density matrices for base isolated bridge.

Mode	Natural frequencies (Hz)		Damping ratio (%)	
	EFDD	SSI	EFDD	SSI
1	0.993	0.995	2.661	3.952
2	1.508	1.505	0.958	0.559
3	2.238	2.241	0.741	0.604
4	2.853	2.874	0.765	2.145
5	3.181	3.258	0.371	0.758
6	4.321	4.298	0.558	0.962

Table 3. Experimentally identified natural frequencies and damping ratios.

http://dx.doi.org/10.5772/64288

Natural frequencies, mode shapes, and damping ratios are given in **Table 3** and **Figure 12**. The first six natural frequencies are obtained between 0.9 and 4.5 Hz. The mode shapes occurred in vertical, torsional, longitudinal, and lateral forms.

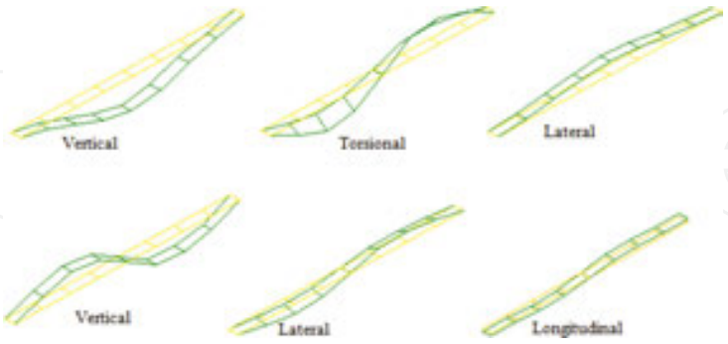


Figure 12. The first six mode shapes of the base isolated bridge.

3.4. Footbridges

Ortahisar and Akçaabat footbridges constructed in Turkey are selected for example. Ortahisar arch-type footbridge is located in a heavy traffic area in Trabzon, Turkey, and has a main span of 35 m. The footbridge operates as part of a pedestrian public footpath [21]. Akçaabat footbridge also operates as part of a pedestrian public footpath [22]. Some views of the footbridges with relieve drawings are given in **Figure 13**.

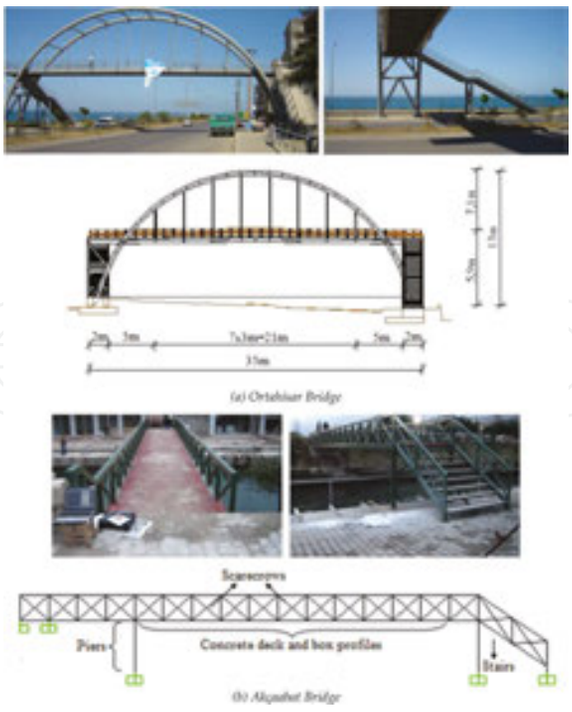


Figure 13. Some views of the footbridges with relieve drawings. (a) Ortahisar Bridge and (b) Akçaabat Bridge.

Some views from the measurements with accelerometer locations are shown in **Figure 14**. The measurements were carried out for at least 45 min. The singular values of spectral density matrices obtained from the processing vibration data are given in **Figure 15**.

The dynamic characteristics such as natural frequencies, mode shapes, and damping ratios obtained using EFDD and SSI methods in frequency and time domain are given in **Table 4** and **Figure 16**. The first six natural frequencies are obtained between 1.9 and 6.7 Hz. The mode shapes occurred in lateral and torsional forms.

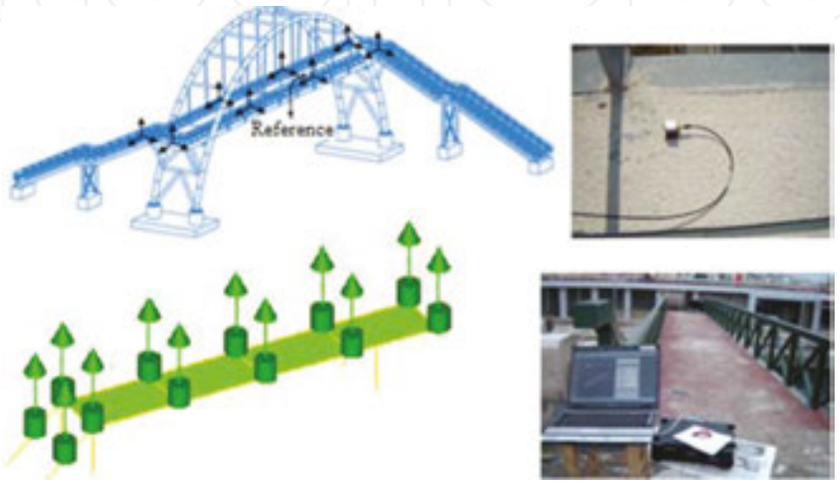


Figure 14. Accelerometer location and views taken from the measurements.

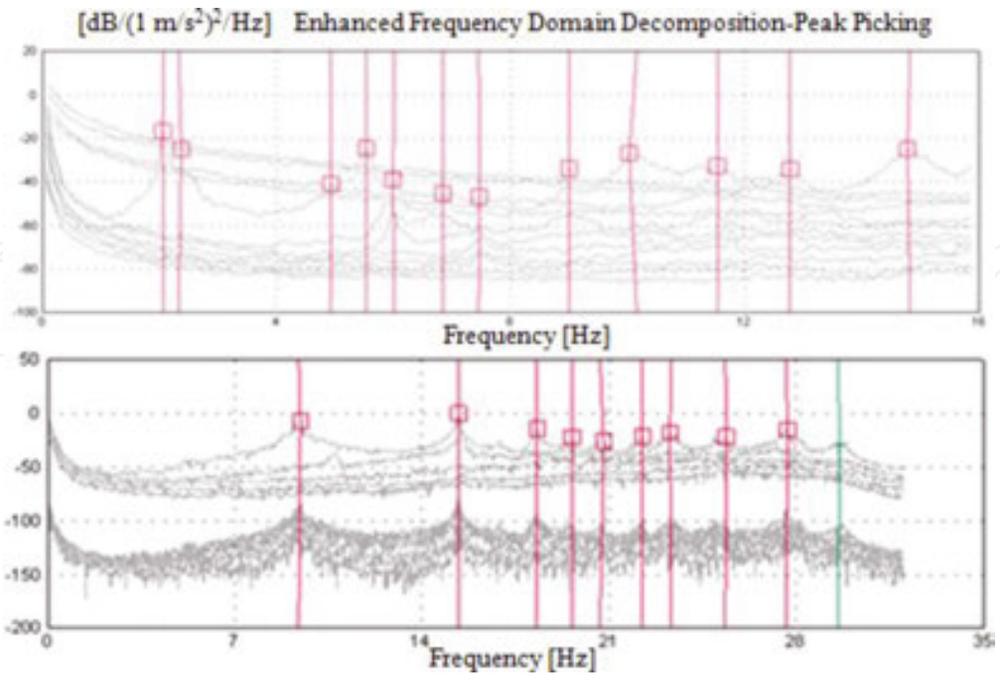


Figure 15. The singular values of spectral density matrices for footbridges.

http://dx.doi.org/10.5772/64288

Mode	Natural frequencies (Hz)		Damping ratio (%)
	EFDD	SSI	
1	2.08	1.90	1.22
2	2.34	2.40	2.82
3	4.78	4.70	0.37
4	5.53	5.50	0.84
5	6.01	5.80	0.40
6	6.67	6.70	0.26

Table 4. Experimentally identified natural frequencies and damping ratios.

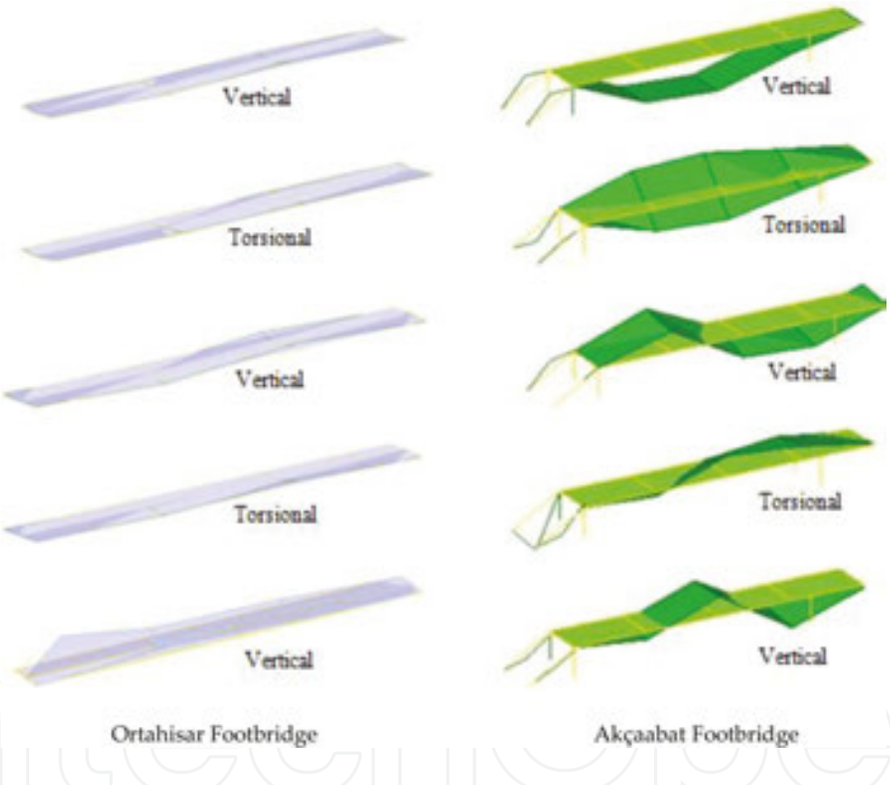


Figure 16. The first five mode shapes of the footbridges.

3.5. Steel bridges

Bridges are one of the most important engineering structures which are commonly used for interplant and intercity transportation. In Turkey, in earlier days they were designed as narrow and short span with stone and wood materials and to be able to carry light loads. Today, the location of these bridges has been replaced with long span reinforced concrete and steel bridges. According to the General Directorate of Highways data, there are 6447 highway bridges with a total length of 296 km in Turkey.

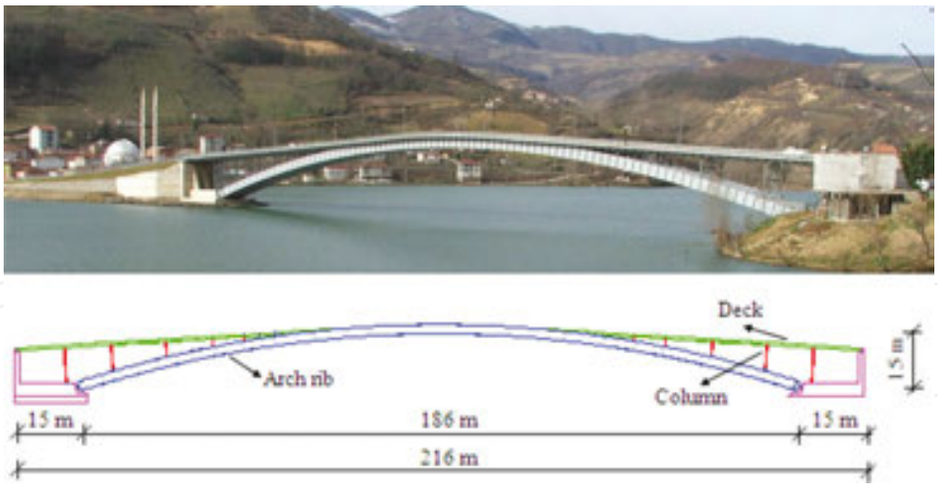


Figure 17. Some views of the steel bridge with relieve drawings.



Figure 18. Accelerometer location and views taken from the measurements.

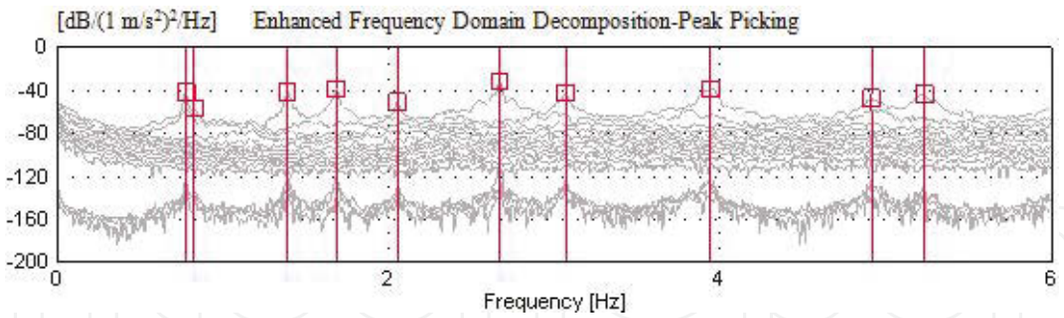


Figure 19. The singular values of spectral density matrices for steel bridge.

Eynel steel bridge constructed in Turkey is selected for example. The bridge is located in the Black Sea region of Turkey. It connects to the villages near the two sides of Suat Uğurlu Dam reservoir in the city of Samsun. The construction of the bridge started in 2007 and it was opened to traffic in 2009. The bridge is upper-deck steel bridge which has arch-type carriage system with a total length of 216 m. The span of the arch rib is 186 m and it has box-type section. The height and width of the section is 2.4 and 12 m. The deck is 12 m wide and has a constant thickness of 10 cm [23]. Some views of the steel bridge are given in **Figure 17**.

In **Figure 18**, the accelerometer locations and views during the measurement are presented in detail. The measurements were carried out for at least 60 min. The singular values of spectral density matrices obtained from the processing vibration data are given in **Figure 19**.

Table 5 and **Figure 20** summarize the dynamic characteristics obtained using EFDD and SSI methods. The first six natural frequencies are obtained between 0.7 and 2.7 Hz. The mode shapes occurred in lateral and transverse forms.

Mode	Natural frequencies (Hz)		Damping ratio (%)	
	EFDD	SSI	EFDD	SSI
1	0.779	0.800	0.73	1.67
2	0.828	-	1.30	-
3	1.395	1.381	0.51	1.06
4	1.688	1.709	0.40	3.26
5	2.057	1.933	0.45	0.84
6	2.674	2.670	0.25	0.36

Table 5. Experimentally identified natural frequencies and damping ratios.

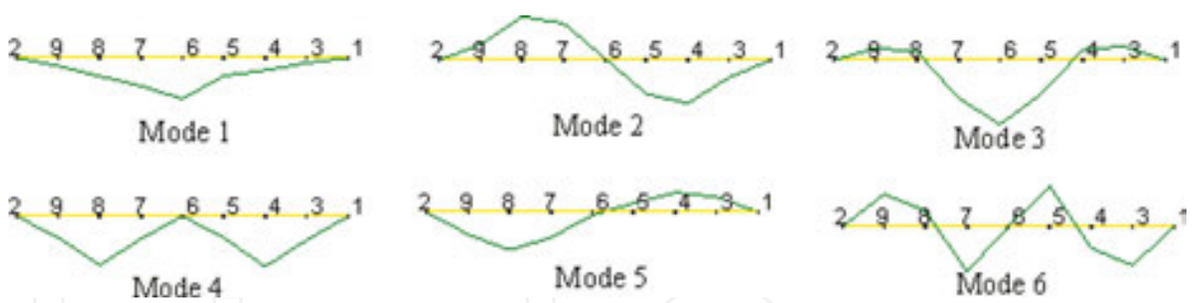


Figure 20. The first six mode shapes of the steel bridge.

3.6. Old riveted bridge

Borçka Old Riveted Bridge constructed in Turkey is selected for example. The bridge, built in 1936, is on the Çoruh River in the town center of Borçka. Total length and width of the bridge are about 114 and 5.30 m, respectively. The main structural system of the bridge has an arch height of 16.30 m from the bridge deck. The bridge girders consist of two edge beams and five middle beams in the longitudinal and transverse directions. The structural elements (arches, pillars, decks, wind connections, etc.) are made out of steel with riveted connections. Bridge is closed to vehicle traffic and it is for only pedestrians [24]. Some views of the old riveted bridge with relieve drawings are given in **Figure 21**.



Figure 21. Some views of the old riveted bridge with relieve drawings.

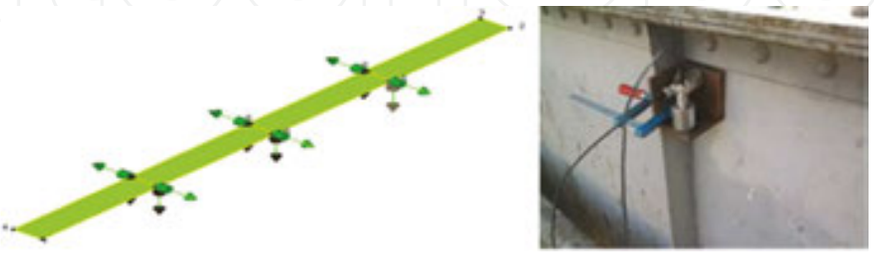


Figure 22. Accelerometer location and views taken from the measurement.

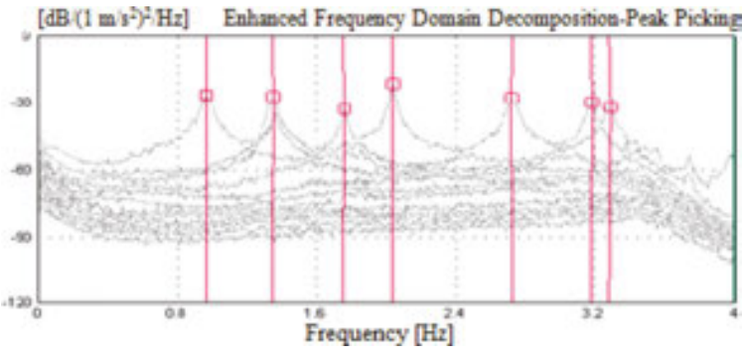


Figure 23. The singular values of spectral density matrices for old riveted bridge.

Mode	Natural frequencies (Hz)		Damping ratio (%)	
	EFDD	SSI	EFDD	SSI
1	0.970	0.968	2.185	1.801
2	1.352	1.348	0.736	0.926
3	1.761	1.758	0.962	0.817
4	2.042	2.041	0.459	0.401
5	2.726	2.725	0.764	0.707
6	3.183	3.189	0.432	0.395

Table 6. Experimentally identified natural frequencies and damping ratios.

http://dx.doi.org/10.5772/64288

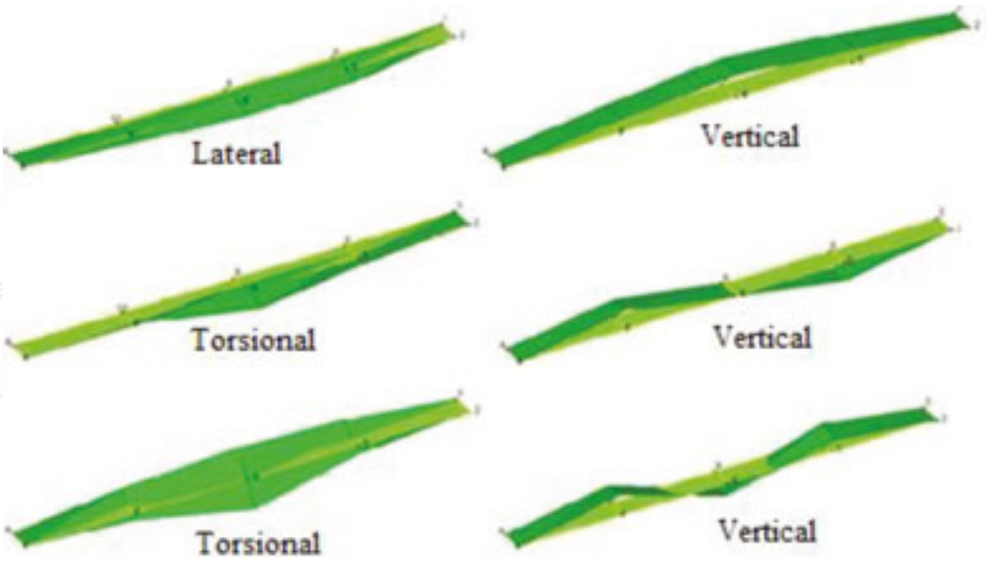


Figure 24. The first six mode shapes of the old riveted bridge.

The accelerometer locations and placements on the deck are displayed in **Figure 22**. The measurements were carried out for at least 60 min. The singular values of spectral density matrices obtained from the vibration data are given in **Figure 23**.

The dynamic characteristics obtained using EFDD and SSI methods are given in **Table 6** and **Figure 24**. The first six natural frequencies are obtained between 0.9 and 3.2 Hz. The mode shapes occurred in lateral, vertical, and torsional forms.

4. Finite element analyses and model updating

To validate the experimentally identified dynamic characteristics, finite element models of the bridges are constituted in the SAP2000 and ANSYS [25, 26] software. With modal analyses, the natural frequencies and related mode shapes are obtained (**Figure 25**). The analytically identified natural frequencies are summarized in **Table 7**.

It is seen that ambient vibration measurements are enough to identify the most significant modes of all bridge types. There is a good agreement between natural frequencies and corresponding mode shapes. The maximum differences are obtained as nearly as 10–20%. To eliminate these differences, the finite element models of the bridges should be updated by changing some uncertain parameters such as material properties, boundary conditions, section areas, etc. It can be evaluated that the maximum differences are reduced from 10–20 to 2–5% after model updating. More information can be found in the literature [11, 12, 15–18, 20–24, 27].

Also, to display the model updating effect, dynamic responses of the bridge are performed before and after model updating. It is seen that this procedure has vital importance to represent the real structural behavior. More information can be found in the literature [11, 12, 15–18, 20–24, 27].

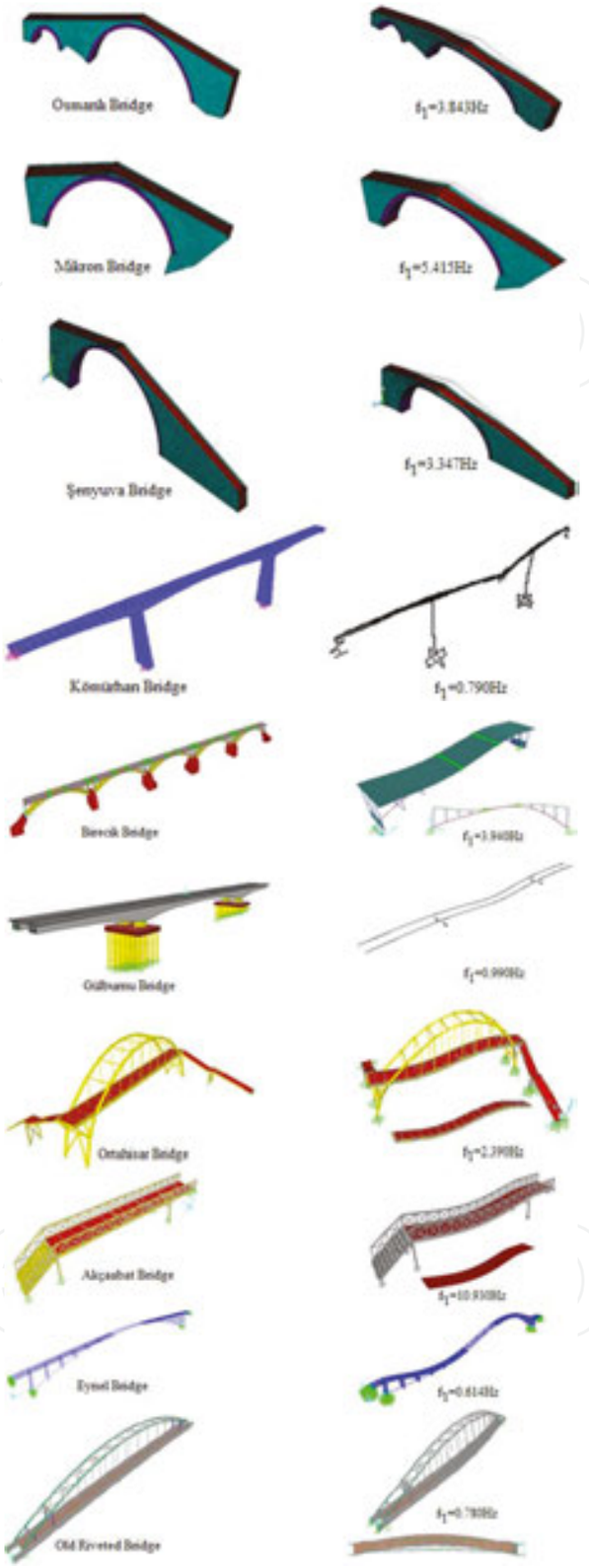


Figure 25. The finite element models of the bridges with first mode shapes.

http://dx.doi.org/10.5772/64288

Bridges		Natural Frequencies					
		1	2	3	4	5	6
Historical masonry	Osmanlı	3.843	7.527	9.371	10.638	14.563	–
	Mikron	5.415	10.113	10.665	13.371	–	–
	Şenyuva	3.347	5.772	7.754	9.055	10.044	–
Long span highway	Kömürhan	0.790	1.106	1.845	2.315	2.685	3.346
	Birecik	3.940	4.770	5.190	8.920	9.530	–
Base isolated	Gülburnu	0.990	1.485	2.164	2.742	3.150	4.186
Footbridge	Ortahisar	2.390	2.500	5.520	5.930	7.630	7.650
	Akçaabat	10.930	15.890	20.810	24.100	33.830	–
Steel	Eynel	0.614	0.718	1.186	1.754	1.940	2.386
Old riveted	Borçka	0.780	1.863	1.960	2.060	2.122	2.930

Table 7. Natural frequencies identified by finite element analyses.

5. Conclusion

This chapter presents a comparative study about the nondestructive measurement of bridges for structural identification. Ten different bridges, which have different type and carrier systems, are selected as case studies. The dynamic characteristics such as natural frequencies, mode shapes, and damping ratios are extracted using ambient vibration tests with operational modal analysis procedure. The experimentally identified dynamic characteristics are validated by the finite element results, and the differences are evaluated.

It can be seen that the ambient vibration measurements are enough to identify the most significant modes of all bridge types.

The first natural frequencies are obtained as 4–14, 0.7–2.3, 2.4–4.6, 0.9–4.5, 1.9–6.7, 0.7–2.7, and 0.9–3.2 Hz for historical masonry arch bridges, Kömürhan and Birecik long span highway bridges, base isolated bridge, footbridges, steel bridges, and old riveted bridges, respectively.

The mode shapes occurred as vertical, lateral, longitudinal, and torsional forms. Especially, longitudinal modes should be considered for a base isolated bridge.

The finite element analyses are performed, and the results are compared with each other. It is seen that there is a good agreement between the natural frequencies and corresponding mode shapes. The maximum differences are nearly within 10–20%.

To eliminate these differences, the finite element models of the bridges should be updated by changing some uncertain parameters such as material properties, boundary conditions, section areas, etc. It can be evaluated that the maximum differences are reduced from 10–20 to 2–5% after model updating procedure. More information can be found in the cited articles.

Acknowledgements

The results presented in this chapter are selected from the author and his co-authors' previous published works. The author was grateful to his advisor Prof. Alemdar Bayraktar and co-authors Assoc. Prof. Barış Sevim and Assist. Prof. Temel Türker for their valuable contributions.

Author details

Ahmet Can Altunışık

Address all correspondence to: ahmetcan8284@hotmail.com

Department of Civil Engineering, Karadeniz Technical University, Trabzon, Turkey

References

[1] Ren WX, Zhao T, Harik IE. Experimental and analytical modal analysis of steel arch bridge. Journal of Structural Engineering. 2004;130(7):1022–1031. DOI: 10.1061/(ASCE)0733-9445.

[2] Jacobsen NJ, Andersen P, Brincker R. Using enhanced frequency domain decomposition as a robust technique to harmonic excitation in operational modal analysis. In: Proceedings of International Conference on Noise and Vibration Engineering (ISMA2006); Leuven, Belgium; 2006.

[3] Bendat JS, Piersol AG. Random Data: Analysis and Measurement Procedures. John Wiley and Sons; USA; 2004.

[4] Brincker R, Zhang L, Andersen P. Modal identification from ambient responses using frequency domain decomposition. In: Proceedings of the 18th International Modal Analysis Conference, San Antonio, USA; 2000.

[5] Felber AJ. Development of hybrid bridge evaluation system. PhD Thesis. Vancouver, Canada: University of British Columbia; 1993.

[6] Peeters B. System identification and damage detection in civil engineering. PhD Thesis. Leuven, Belgium: K.U; 2000.

[7] Peeters B, DeRoeck G. Reference based stochastic subspace identification in civil engineering. In: Proceedings of the 2nd International Conference on Identification in Engineering Systems; Swansea, UK; 1999. Pp. 639–648.

[8] Ewins DJ. Modal Testing: Theory and Practice. England: Research Studies Press Ltd; 1984.

[9] Juang JN. Applied System Identification. Englewood Cliffs, NJ: Prentice-Hall Inc; 1994.

[10] Allemang RJ. The modal assurance criterion: twenty years of use and abuse. Sound and Vibration. 2003;37(8):14–23.

[11] Bayraktar A, Birinci F, Altunışık AC, Türker T, Sevim B. Finite element model updating of Senyuva historical arch bridge using ambient vibration tests. The Baltic Journal of Road and Bridge Engineering. 2009;4(4):177–185. DOI: 10.3846/1822-427X. 2009.4.177-185.

[12] Sevim B, Bayraktar A, Altunışık AC, Atamtürktür S, Birinci F. Assessment of nonlinear seismic performance of a restored historical arch bridge using ambient vibrations. Nonlinear Dynamics. 2011;63(4);755–770. DOI: 10.1007/s11071-010-9835-y.

[13] PULSE. Analyzers and Solutions. Release 11.2. Bruel and Kjaer; Sound and Vibration Measurement A/S; Denmark; 2006.

[14] OMA. Operational Modal Analysis. Release 4.0. Bruel and Kjaer; Structural Vibration Solutions A/S; Denmark; 2006.

[15] Brownjohn JMW, Magalhaes F, Caetano E, Cunha A. Ambient vibration re-testing and operational modal analysis of the Humber Bridge. Engineering Structures. 2010;32:2003–2018. DOI: 10.1016/j.engstruct.2010.02.034.

[16] Bayraktar A, Altunışık AC, Sevim B, Türker T. Earthquake behaviour of kömürhan highway bridge using validated finite element model. Journal of Testing and Evaluation. 2010;38(4):467–481. DOI: 10.1520/JTE102102.

[17] Bayraktar A, Altunışık AC, Sevim B, Türker T. Finite element model updating of Kömürhan highway bridge based on experimental measurements. Journal of Smart Structures and Systems. 2010;6(4):373–388. DOI: 10.12989/sss.2010.6.4.373.

[18] Bayraktar A, Altunişik AC, Türker T. Structural condition assessment of Birecik Highway Bridge using operational modal analysis. International Journal of Civil Engineering. 2016;13(5):1–30.

[19] Ateş Ş, Constantinou MC. Example of application of response history analysis for seismically isolated curved bridges on drilled shaft with springs representing soil. Soil Dynamics and Earthquake Engineering. 2011;31(3):334–350. DOI: 10.1016/j.soildyn. 2010.09.002.

[20] Altunışık AC, Bayraktar A, Sevim B. Output-only system identification of post tensioned segmental concrete highway bridges. Journal of Bridge Engineering. 2011;16(2):259–266. DOI: 10.1061/(ASCE)BE.1943-5592.0000150.

[21] Bayraktar A, Altunışık AC, Sevim B, Türker T. Modal testing, finite element model updating and dynamic analysis of an arch type steel footbridge. Journal of Performance of Constructed Facilities. 2009;23(2):81–89. DOI: 10.1061/(ASCE)0887-3828.

[22] Bayraktar A, Altunışık AC, Sevim B, Türker T. Ambient vibration tests of a steel footbridge. Journal of Nondestructive Evaluation. 2010;29(1):14–24. DOI: 10.1007/s10921-009-0061-9.

[23] Altunışık AC, Bayraktar A, Sevim B, Özdemir H. Experimental and analytical system identification of Eynel arch type steel highway bridge. Journal of Constructional Steel Research. 2011;67(12):1912–1921.

[24] Bayraktar A, Altunışık AC, Türker T. Structural health assessment and restoration procedure of an old riveted steel arch bridge. Soil Dynamics and Earthquake Engineering. 2016; 83:148–161. DOI: 10.1016/j.soildyn.2016.01.012.

[25] SAP2000. Integrated Finite Element Analysis and Design of Structures. Berkeley, CA, USA: Computers and Structures Inc.; 1998.

[26] ANSYS. Swanson Analysis System. USA; 2003.

[27] Sevim B, Atamturktur S, Altunışık AC, Bayraktar A. Ambient vibration testing and seismic behavior of historical arch bridges under near and far fault ground motions. Bulletin of Earthquake Engineering. 2016;14:241–259. DOI: 10.1007/s10518-015-9810-6.

IntechOpen